The organ-specific perfusion response to adenosine as measured using total-body positron emission tomography

Henri Kärpijoki[1], Jouni Tuisku[1], Santeri Palonen[1], Chunlei Han[1], Hidehiro Iida[1], Riku Klén[1], Vesa Oikonen[1], Jarmo Teuho[1], Antti Saraste[1,2], Lauri Nummenmaa[1,3], Sergey V. Nesterov[1], Teemu Maaniitty[1,4], Juhani Knuuti[1,4]

[1]Turku PET Centre, Turku University Hospital, and University of Turku, Turku, Finland

[2]Heart Center, Turku University Hospital, and University of Turku, Turku, Finland

[3]Department of Psychology, University of Turku, Turku, Finland

[4]Department of Clinical Physiology, Nuclear Medicine, and PET, Turku University Hospital, Turku, Finland

Keywords: $[^{15}O]H_2O$, adenosine, flow, long axial field of view PET

Short title: Adenosine response by total-body PET

Word count: xx

ClinicalTrials.gov ID NCT05825859, **Total Body Perfusion in Patients With Chest Pain (KOVERI), Study start date April 11, 2023**

Corresponding author:

Henri Kärpijoki

Turku PET Centre, Turku University Hospital, and University of Turku

Po Box 52, 20521 Turku, Finland

Email: hjkarp@utu.fi

ORCID: 0009-0005-4152-9490

Abstract

Purpose: Adenosine is routinely used as a pharmacological stressor in myocardial perfusion imaging, but its effects on other organs have not been comprehensively studied. The aim of this study was to investigate the effect of adenosine on the perfusion of different organs using a long axial field of view positron emission tomography (LAFOV-PET) scanner.

Methods: We included 91 patients who were prospectively recruited to undergo LAFOV-[^{15}O]H_2O PET perfusion imaging at rest and during adenosine stress with suspected coronary artery disease and who did not have myocardial ischemia or prior stroke. Analysis was performed using an in-house open-source TURBO-pipeline, including computed tomography -based segmentation of organs other than the heart. Organ-specific absolute perfusion values were measured.

Results: Adenosine increased global myocardial blood flow, with a median of 1.01 [25th-75th percentiles 0.90–1.22] mL/min/g at rest, and 3.47 [3.06–3.95] mL/min/g at stress. Perfusion in other organs was measured in mL/min/mL and was increased during stress in the liver (rest: 1.10 [0.83–1.82], stress: 3.32 [1.79–5.41], p<0.0001), duodenum (rest: 0.37 [0.27–0.48], stress: 0.53 [0.42–0.65], p<0.0001), and colon (rest: 0.09 [0.08–0.12], stress: 0.13 [0.10–0.17], p<0.0001). In contrast, perfusion decreased in the brain (rest 0.43 [0.38–0.48], stress 0.32 [0.28–0.35], p<0.0001), and kidneys (rest 0.87 [0.75–1.00] mL/min/mL, stress 0.65 [0.49–0.76], p<0.0001). In the spleen, perfusion was reduced by 71% as a sign of splenic switch-off (rest 1.11 [0.97–1.30], stress 0.31 [0.23–0.40], p<0.0001).

Conclusion: The perfusion response to adenosine is organ-specific. In the heart, liver, colon, and duodenum, perfusion is increased by adenosine, but in the brain, spleen, and kidneys, the perfusion is reduced. Our results highlight the systemic nature of adenosine effects.

Introduction

Long axial field of view positron emission tomography (LAFOV-PET) scanners allow simultaneous dynamic imaging of all the internal organs and major tissues, with the potential to study the function of and interactions between different body organs. Oxygen-15-labelled water ([^{15}O]H_2O) is an established tracer for quantitative myocardial perfusion imaging, and in combination with total-body PET scanners, it is promising method for investigating perfusion in different organs as well as their interactions[1].

Adenosine is widely used as a pharmacological stressor in myocardial perfusion imaging. Variable vasodilating or vasoconstrictive effects of adenosine have been reported. In the heart, adenosine causes vasodilatation, whereas in the spleen it causes vasoconstriction[2,3]. The latter is known as a splenic switch-off phenomenon that has been proposed as a tool to evaluate the adequacy of pharmacological stress in cardiac imaging[3,4]. However, limited data exist on the adenosine response in the other body organs[5–8].

Here we used quantitative LAFOV-PET to measure perfusion at rest and during adenosine stress in the heart, liver, spleen, kidneys, brain, colon, duodenum, bone, and skeletal muscle in patients without ischemic heart disease or a history of stroke. Our goal was to assess the organ-specific effects of adenosine.

Materials and methods

Study cohort.

We prospectively recruited 191 patients to undergo rest and adenosine stress total-body PET perfusion imaging with [^{15}O]H_2O at the Turku University Hospital between August 2022 and February 2025. The patients had been originally referred for a myocardial PET perfusion scan for evaluation of suspected obstructive coronary artery disease (CAD), mostly triggered by the presence of coronary atherosclerosis on coronary computed tomography (CT) angiography. After exclusion of 15 patients with incomplete or missing data, 176 patients were successfully analysed (**Supplemental Figure 1**). Out of these, we excluded 76 patients with abnormal myocardial stress perfusion (n = 76) and additional 9 patients due to history of stroke, resulting in a final cohort of 91 patients.

The clinical data were recorded from the medical records and patient interviews (type of symptoms, cardiovascular risk factors including smoking, hypertension, dyslipidaemia, diabetes, family history of CAD, and a history of stroke).

Brachial blood pressure, weight, and height were measured. Agatston coronary artery calcium score was recorded if it had been measured within a year prior to the PET-imaging.

The study complies with the Declaration of Helsinki. The Ethics Committee of the Hospital District of Southwest Finland approved the study protocol. Written informed consent was obtained from all patients. The study has been registered in ClinicalTrials.gov (NCT05825859).

PET image acquisition

Patients underwent total-body [^{15}O]H_2O PET imaging using Siemens Biograph Vision Quadra PET/CT (Siemens Healthineers). Patients were instructed to abstain from caffeine for 24 hours prior to the PET scan. A single low-dose total-body CT scan of $512 \times 512 \times 380$ voxels of $0.977 \times 0.977 \times 3.00$ mm^3 was first acquired. The rest PET scan was followed by an adenosine stress PET scan, with a minimum of 10 min time interval between acquisitions. For both rest and stress scans, [^{15}O]H_2O tracer (Radiowater Generator, Hidex Oy, Turku, Finland) was injected as an intravenous bolus (target activity 350 MBq ± 10 %) of approximately 5 seconds. Dynamic PET acquisition, with a total imaging time of 4 minutes and 40 seconds, was initiated 30 seconds after the tracer administration. The data were reconstructed into 14 frames of 5 seconds, followed by 3 frames of 10 seconds, 3 frames of 20 seconds, and 4 frames of 30 seconds. All images were reconstructed using UltraHD-PET in High Sensitivity mode. The first reconstruction used three iterations and five subsets with a matrix size of 220 or 440, a zoom factor of 2.0, and a Gaussian filter of 3.0 mm. The second reconstruction employed four iterations, a zoom factor of 1.0, and a Gaussian filter of 4.0 mm. Data were corrected for attenuation, scatter, randoms, and decay. Adenosine infusion was started 2 minutes before the stress PET scan and continued at a rate of 140 µg/kg/min until the scan was complete. Blood pressure and heart rate were recorded at rest and after 3 minutes of adenosine infusion.

PET image analysis

Heart

The heart was analysed using the cardiac analysis software Carimas (Turku PET Centre, Turku, Finland) [9,10] using the standard myocardial model [11]. The heart was segmented into 17 myocardial segments for which absolute rest and stress myocardial blood flow (MBF) in mL/min/g was quantified based on k2 using a one-tissue compartment model with left ventricular time-activity curve as the arterial input function, where the effects of the systemic underestimation in the left ventricular signal and the spillover from the myocardial radioactivity were taken into account [9,11]. Global MBF was also calculated as well as territorial MBF in the left ascending coronary artery (LAD), left circumflex artery (LCX), and right coronary artery (RCA). Patients with myocardial ischemia, defined as the presence of ≥2 adjacent myocardial segments with stress MBF below 2.3 mL/g/min, were excluded from the analysis [12].

Brain

The brain was segmented into grey and white matter compartments using the Magia-toolbox that extracts the brain from the original PET image, corrects the motion rigidly and normalises it into a template [13]. The method has been previously described in detail [14].

Other organs

Segmentation of the other organs was performed using a CT-based total body segmentation method TotalSegmentator [15] implemented in the TURBO total body analysis pipeline described and validated earlier [1,14]. Iliopsoas was chosen to represent skeletal muscle and femur to represent bone (including bone marrow). Segmented organs were analysed using one-tissue compartment model with descending aorta input function, except in the liver [16], where the model input was combined using the estimated portal vein [17] in addition to the descending aorta input function [14]. The blood flow was quantified as flow=(1-Va)*K1 in units mL/min/mL, representing the organ perfusion, and additionally, k2 (1/min) and arterial blood volume (Va) were estimated [14]. Input function was extracted from the descending aorta automatically using a previously validated method [14].

Statistical analysis

Continuous variables are reported as mean and standard deviation (SD) or median [interquartile range (IQR): 25^{th}–75^{th} percentiles] as appropriate. Categorical variables are shown as counts (percentage). Wilcoxon signed-rank test was used to compare the stress versus rest conditions in different organs. Paired t-test was used to compare blood pressures and heart rates at rest and after 3 minutes of adenosine infusion. Multiple testing was corrected for with the Benjamini-Hochberg false discovery rate -method. In the bilateral organs such as the kidney, skeletal muscle, and femur, data was averaged across left and right sides. The statistical analyses were performed using R software, version 4.3.2 (R Foundation for Statistical Computing) [18]. The threshold for statistical significance was 2-tailed $p<0.05$.

Results

Study cohort

TABLE 1 shows baseline characteristics of the 91 patients included in the study. In this selected cohort of patients without myocardial ischemia or a history of stroke, the majority (71%) of patients were female. There was a significant increase in heart rate (rest mean 66.5 (11.6), stress 87.4 (14.4), $p<0.0001$) and decrease in diastolic blood pressure (rest 71.1 (12.5), stress 66.1 (13.5), $p<0.0001$) from rest to 3-minute stress. However, systolic blood pressure did not significantly differ between rest and 3-minute stress ($p=0.14$).

Myocardial perfusion

The global and territorial MBF at rest and during stress are shown in **TABLE 2** and **Figure 1.** By definition of our study cohort (i.e., patients with myocardial ischemia were excluded), there was a more than 3-fold increase ($p<0.0001$) in MBF during adenosine infusion globally and in the main coronary artery territories. We observed significant differences in MBF between vascular territories at rest and during adenosine stress.

Figure 1 Myocardial blood flow (MBF) at rest and during adenosine stress in the whole left ventricular myocardium and in each main coronary artery territory

LAD = Left anterior descending artery, LCX = left circumflex artery, RCA = right coronary artery

Figure 1 shows a ~3-fold increase ($p<0.0001$) in myocardial perfusion in each main coronary artery territory. There also appear to be some outliers showing unexpectedly high rest MBF.

Perfusion in other organs

TABLE 3 shows the quantified perfusion in different organs at rest and during stress as well as stress/rest ratio (reserve), and the difference between stress and rest (delta). **Figure 2** demonstrates individual changes in perfusion in each organ. In the whole brain, white matter, and cortical grey matter there were statistically significant ($p<0.0001$) reductions in perfusion induced by adenosine. There was also a perfusion reduction in skeletal muscle ($p<0.0001$), spleen ($p<0.0001$), kidneys ($p<0.0001$), and bone ($p<0.0001$).

There was an adenosine-induced increase in perfusion in the liver ($p<0.0001$), colon ($p<0.0001$), and duodenum ($p<0.0001$). The distribution volume (rest median 0.71 [0.68–0.76], stress 0.69 [0.64–0.74], $p=0.0015$) showed less variance in the liver as compared to flow and k2. The pancreas did not show a significant difference in perfusion between rest and stress. Outliers were observed in multiple organs; however, they are from different patients for different organs expect for one patient who had unexpectedly high rest MBF in addition to high flow in colon and spleen at rest and during stress.

The k2 and Va results are shown on **supplemental TABLEs 1** and **2** and **supplemental Figure 2** and **Figure 3**.

Discussion

In this prospective cohort study, we demonstrated that adenosine-induced perfusion responses are highly organ-specific, with both vasodilatory and vasoconstrictive effects evident across the body. Using LAFOV [^{15}O]H_2O PET imaging, we were able to simultaneously and quantitatively assess perfusion in multiple organs under pharmacological stress by intravenous adenosine. These findings highlight the systemic effects of adenosine and the potential of LAFOV-PET for functional flow imaging beyond the myocardium.

Myocardial response and splenic switch-off

As expected, in this selected study cohort without myocardial ischemia, adenosine induced a robust increase in MBF, in line with established literature on coronary vasodilation. Adenosine caused an over 3-fold increase in myocardial perfusion compared with the resting state, as seen in other studies including patients without obstructive CAD [3,9,19]. By definition, the MBF values observed during adenosine stress were above the established ischemic threshold [12] in all patients, ascertaining the adequacy of pharmacological stress and the integrity of coronary vasodilatory capacity in this cohort. Notably, response to adenosine was similar to previous studies reporting reference ranges of stress MBF and myocardial flow reserve [19] despite relatively high prevalence of cardiovascular risk factors and coronary atherosclerosis in our cohort. The patient selection in this study was justified by the fact that we wanted to evaluate organ-specific effects of adenosine in a “reference” population without flow-limiting CAD, whereas patients with myocardial ischemia might have perfusion changes in other organs as well, even though this remains to be investigated in future studies. Similarly, we excluded patients with abnormalities in brain perfusion or clinical history of cerebrovascular disease. Moreover, by focusing on patients with adequate adenosine-induced increase in myocardial perfusion, we can make sure that there is no system-level lack of adenosine response, for example, due to caffeine consumption.

Notably, the spleen demonstrated a substantial reduction in perfusion, consistent with the splenic switch-off phenomenon in multiple previous studies [3,4,7]. This inverse response has previously been proposed as an indicator of sufficient adenosine effect and was clearly observed here, reinforcing its potential clinical utility as a systemic marker of stress adequacy.

Perfusion heterogeneity across organs

Interestingly, adenosine significantly increased perfusion in the liver, colon, and duodenum, while it decreased perfusion in the brain, kidneys, skeletal muscle, and bone.

The reduction of brain perfusion aligns with prior studies showing that systemic adenosine can paradoxically reduce cerebral blood flow, likely due to systemic hypotension, or respiratory effects. This observation might also reflect different adenosine receptor expression and regulation in cerebral versus coronary vascular beds.

There are no large studies on adenosine effects in the brain. In one study, the cerebral blood flow (CBF) was measured using ^{133}Xe single-photon emission computed tomography imaging and adenosine had no statistically significant effect on brain perfusion [20]. In another study, there was no difference in cerebral blood flow after adenosine infusion measured using magnetic resonance imaging (MRI) and [^{15}O]Butanol PET imaging[21]. However, when large doses of adenosine (200-500 µg/kg/min) were given in six patients under general anaesthesia and when ventilation was controlled, a large increase in global CBF was seen without correlation with adenosine doses [22].

In a small study with 13 healthy subjects, dipyridamole decreased brain perfusion when measured by [^{15}O]H_2O PET and it was closely followed by changes in hypocapnia [23]. Adenosine is known to induce hyperventilation via chemoreceptor stimulation [24]. In turn, hyperventilation causes hypocapnia and vasoconstriction, therefore reducing brain perfusion, as also seen in the present study. The magnitude for resting perfusion in cortical grey matter, white matter, and the whole brain was comparable to healthy subjects measured in other studies [25–28].

The hepatic response, characterised by a substantial increase in perfusion, may reflect combined hepatic arterial vasodilation and portal flow augmentation, possibly involving the hepatic arterial buffer response. The liver perfusion is relatively difficult to model because both the hepatic artery and the portal vein provide blood to the liver. The liver controls the blood supply via the hepatic artery because the portal vein blood flow cannot be directly controlled [29]. Prior studies using PET and MRI have reported similar findings under adenosine stress, supporting the reproducibility of our observations [7,30]. The hepatic perfusion has been studied using ^{82}Rb-PET/CT imaging on 45 patients with clinical indications for cardiovascular imaging. In that study, it was found that hepatic arterial perfusion approximately doubled after over 6 min of adenosine infusion [7], that is in agreement with our study.

Renal perfusion was significantly reduced, in agreement with earlier findings of adenosine-induced afferent arteriolar vasoconstriction in the kidney [8,31]. These results are consistent with the known role of adenosine in tubuloglomerular feedback and emphasise the kidney's unique response pattern. The kidney involves two functionally different regions, the cortex and the medulla. We segmented the kidney as a whole, although the perfusion in these regions might differ.

The increase in gastrointestinal perfusion (colon and duodenum) may be attributed to adenosine receptor-mediated vasodilation within the splanchnic circulation. This has physiological relevance in contexts of digestive or pharmacological hyperaemia but remains under-investigated in clinical imaging and the perfusion during adenosine stress in the colon and duodenum has not been previously studied in humans.

The observed decrease in skeletal muscle and bone perfusion during stress may reflect systemic redistribution of blood flow toward vasodilated vascular beds, though further mechanistic studies are needed. The previously published perfusion results for the skeletal muscles at rest are similar to our study [32,33], but adenosine stress has been shown [34,35] to increase muscle perfusion. In earlier studies, the perfusion of the quadriceps femoris muscle has been measured instead of the iliopsoas used in the current study. We chose the iliopsoas as the patients may contract the quadriceps muscle due to the symptoms caused by adenosine. The decrease in bone perfusion [36] has also been shown previously.

Methodological Considerations

Our study leveraged the high sensitivity and resolution of a long axial field-of-view PET system, combined with robust CT-based organ segmentation and validated kinetic modelling pipelines. This allowed for precise, reproducible quantification of perfusion across anatomically distinct tissues. Nevertheless, several limitations should be considered.

First, the study cohort consisted of symptomatic patients referred for evaluation of suspected coronary artery disease, albeit without myocardial ischemia, and may not represent healthy individuals. Second, potential confounding effects of medications, comorbidities, or systemic hemodynamics were not fully controlled, though relatively large sample size helps to mitigate interindividual variability. Third, although the subjects were asked to abstain from caffeine-containing beverages for 24 hours before the PET study, we cannot rule out caffeine effects, as it was not measured. However, patients with normal stress myocardial perfusion were included in the analysis, and therefore, a blunted effect of adenosine is unlikely. Fourth, most of the organs were analysed using a one-tissue compartment model, but some organs may need more sophisticated organ-specific models. E.g., in liver calculations of dual input function [6,17] we accounted the dual blood supply to the liver by estimating the portal vein input function. Also, the applied TURBO pipeline's kidney modelling may underestimate later-phase time activity curves due to the kinetic model being oversimplified, missing tubular reabsorption/excretion [37], as well as an additional input from the efferent vessels to the reuptake site. Cortex-tubule heterogeneity may distort kinetics [38], while motion sensitivity might worsen errors. These more nuanced models should be developed and implemented in future studies. Fifth, women were overrepresented in our study cohort which may be because women generally have higher myocardial blood flow and lower prevalence of ischemic CAD. Additionally, while $[^{15}O]H_2O$ is a gold-standard perfusion tracer for the tissues where the tracer is distributed instantaneously to the equilibrium through the capillary system, this is likely not the case in several organs, e.g., in the kidneys. The partial volume effects and motion artifacts, especially in small or mobile organs, may influence quantification.

Clinical relevance and future directions

Our results highlight the systemic nature of adenosine effects and suggest that organ-specific perfusion responses can be leveraged for broader functional assessments. For example, the consistent splenic switch-off may serve as a surrogate marker of adenosine efficacy. Likewise, the differential response of the liver and gastrointestinal tract may open avenues for assessing hepatic perfusion reserve or inflammatory bowel conditions. Furthermore, understanding of physiological processes detected by LAFOV PET is a prerequisite for implementing this methodology into investigating mechanisms of novel drug therapies (such as SGLT2 inhibitors) that have demonstrated beneficial effects in multiple organs.

Future studies should investigate multi-organ perfusion in healthy volunteers and specific patient populations (e.g., liver disease, neurovascular disorders) and explore the utility of multi-organ perfusion profiling for disease characterisation and treatment monitoring. Moreover, the integration of perfusion, distribution volume as a marker of the water-prefusable tissue fraction, and metabolic imaging (e.g., FDG-PET) could offer comprehensive insight into organ function in vivo.

Conclusions

The perfusion response to adenosine appears organ-specific. Adenosine increases perfusion in the heart, liver, colon, and duodenum, whereas perfusion is reduced by adenosine in the brain, spleen, kidneys, skeletal muscle, and bone. Our results highlight the systemic nature of adenosine effects and the potential of LAFOV PET for simultaneous assessment of multi-organ perfusion.

Disclosure of interest

This work was supported by the European Research Council (Advanced Grant #101141656 to LN), Jane and Aatos Erkko Foundation, the Finnish Foundation for Cardiovascular Research, Finnish State Research Funding (VRT), Finnish Cultural Foundation, InFLAMES research flagship and Gyllenberg's Stiftelse. Dr. Maaniitty received research funding from the Research Council of Finland. Jarmo Teuho was funded by the Research Council of Finland, Academy Research Fellowship grant #360120.

Dr. Knuuti has received consultancy fees from GE Healthcare and Synektik and speaker fees from Siemens Healthineers, outside of the submitted work. Dr Saraste has received consultancy or speaker fees from Abbott, Astra Zeneca, BMS, Janssen, Novo Nordisk, and Pfizer outside the submitted work.

List of figures and tables

Figures

Figure 1: **Figure 1** Myocardial blood flow (MBF) at rest and during adenosine stress in the whole left ventricular myocardium and in each main coronary artery territory

Figure 2: Perfusion (flow) values in different organs at rest and during adenosine stress

Tables

TABLE 1: Baseline characteristics of patients (n = 91)

TABLE 2: Myocardial blood flow (MBF) in the left ventricular myocardium and in each main coronary artery territory

TABLE 3: Perfusion at rest and during stress in different organs

References

1. Knuuti J, Tuisku J, Kärpijoki H, et al. Quantitative Perfusion Imaging with Total-Body PET. *J Nucl Med*. 2023;64(Suppl 2):11S-19S. doi:10.2967/jnumed.122.264870

2. Knuuti J, Ballo H, Juarez-Orozco LE, et al. The performance of non-invasive tests to rule-in and rule-out significant coronary artery stenosis in patients with stable angina: a meta-analysis focused on post-test disease probability. *European Heart Journal*. 2018;39(35):3322-3330. doi:10.1093/eurheartj/ehy267

3. Inkinen SI, Hippeläinen E, Uusitalo V. Adenosine-induced splenic switch-off on [15O]H2O PET perfusion for the assessment of vascular vasodilatation. *EJNMMI Res*. 2023;13(1):96. doi:10.1186/s13550-023-01045-7

4. Manisty C, Ripley DP, Herrey AS, et al. Splenic Switch-off: A Tool to Assess Stress Adequacy in Adenosine Perfusion Cardiac MR Imaging. *Radiology*. 2015;276(3):732-740. doi:10.1148/radiol.2015142059

5. Pelletier-Galarneau M, deKemp RA, Hunter CRRN, et al. Effects of Hypercapnia on Myocardial Blood Flow in Healthy Human Subjects. *J Nucl Med*. 2018;59(1):100-106. doi:10.2967/jnumed.117.194308

6. Ziegler SI, Haberkorn U, Byrne H, et al. Measurement of liver blood flow using oxygen-15 labelled water and dynamic positron emission tomography: limitations of model description. *Eur J Nucl Med*. 1996;23(2):169-177. doi:10.1007/BF01731841

7. Keramida G, Gregg S, Peters AM. Stimulation of the hepatic arterial buffer response using exogenous adenosine: hepatic rest/stress perfusion imaging. *Eur Radiol*. 2020;30(11):5852-5861. doi:10.1007/s00330-020-06984-6

8. Vallon V, Mühlbauer B, Osswald H. Adenosine and kidney function. *Physiol Rev*. 2006;86(3):901-940. doi:10.1152/physrev.00031.2005

9. Nesterov SV, Han C, Mäki M, et al. Myocardial perfusion quantitation with 15O-labelled water PET: high reproducibility of the new cardiac analysis software (Carimas). *Eur J Nucl Med Mol Imaging*. 2009;36(10):1594-1602. doi:10.1007/s00259-009-1143-8

10. Rainio O, Han C, Teuho J, et al. Carimas: An Extensive Medical Imaging Data Processing Tool for Research. *J Digit Imaging*. 2023;36(4):1885-1893. doi:10.1007/s10278-023-00812-1

11. Cerqueira MD, Weissman NJ, Dilsizian V, et al. Standardized myocardial segmentation and nomenclature for tomographic imaging of the heart. A statement for healthcare professionals from the Cardiac Imaging Committee of the Council on Clinical Cardiology of the American Heart Association. *Circulation*. 2002;105(4):539-542. doi:10.1161/hc0402.102975

12. Danad I, Uusitalo V, Kero T, et al. Quantitative assessment of myocardial perfusion in the detection of significant coronary artery disease: cutoff values and diagnostic accuracy of quantitative [(15)O]H2O PET imaging. *J Am Coll Cardiol*. 2014;64(14):1464-1475. doi:10.1016/j.jacc.2014.05.069

13. Karjalainen T, Tuisku J, Santavirta S, et al. Magia: Robust Automated Image Processing and Kinetic Modeling Toolbox for PET Neuroinformatics. *Front Neuroinform*. 2020;14:3. doi:10.3389/fninf.2020.00003

14. Tuisku J, Palonen S, Kärpijoki H, et al. Automated Total-body PET Image Processing and Kinetic Modeling with the TURBO Toolbox. Preprint posted online June 9, 2025. doi:10.1101/2025.06.06.658206

15. Wasserthal J, Breit HC, Meyer MT, et al. TotalSegmentator: Robust Segmentation of 104 Anatomic Structures in CT Images. *Radiol Artif Intell*. 2023;5(5):e230024. doi:10.1148/ryai.230024

16. Lammertsma AA. Radioligand studies: imaging and quantitative analysis. *Eur Neuropsychopharmacol*. 2002;12(6):513-516. doi:10.1016/s0924-977x(02)00100-1

17. Kudomi N, Slimani L, Järvisalo MJ, et al. Non-invasive estimation of hepatic blood perfusion from H2 15O PET images using tissue-derived arterial and portal input functions. *Eur J Nucl Med Mol Imaging*. 2008;35(10):1899-1911. doi:10.1007/s00259-008-0796-z

18. R Core Team (2023). _R: A Language and Environment for Statistical Computing_. R Foundation for Statistical Computing, Vienna, Austria. <https://www.R-project.org/>.

19. Murthy VL, Bateman TM, Beanlands RS, et al. Clinical Quantification of Myocardial Blood Flow Using PET: Joint Position Paper of the SNMMI Cardiovascular Council and the ASNC. *J Nucl Med*. 2018;59(2):273-293. doi:10.2967/jnumed.117.201368

20. Birk S, Petersen KA, Kruuse C, et al. The effect of circulating adenosine on cerebral haemodynamics and headache generation in healthy subjects. *Cephalalgia*. 2005;25(5):369-377. doi:10.1111/j.1468-2982.2005.00867.x

21. Stånge K, Greitz D, Ingvar M, Hindmarsh T, Sollevi A. Global cerebral blood flow during infusion of adenosine in humans: assessment by magnetic resonance imaging and positron emission tomography. *Acta Physiol Scand*. 1997;160(2):117-122. doi:10.1046/j.1365-201X.1997.00113.x

22. Sollevi A, Ericson K, Eriksson L, Lindqvist C, Lagerkranser M, Stone-Elander S. Effect of adenosine on human cerebral blood flow as determined by positron emission tomography. *J Cereb Blood Flow Metab*. 1987;7(6):673-678. doi:10.1038/jcbfm.1987.121

23. Ito H, Kinoshita T, Tamura Y, Yokoyama I, Iida H. Effect of intravenous dipyridamole on cerebral blood flow in humans. A PET study. *Stroke*. 1999;30(8):1616-1620. doi:10.1161/01.str.30.8.1616

24. Biaggioni I, Olafsson B, Robertson RM, Hollister AS, Robertson D. Cardiovascular and respiratory effects of adenosine in conscious man. Evidence for chemoreceptor activation. *Circ Res*. 1987;61(6):779-786. doi:10.1161/01.res.61.6.779

25. Aanerud J, Borghammer P, Rodell A, Jónsdottir KY, Gjedde A. Sex differences of human cortical blood flow and energy metabolism. *J Cereb Blood Flow Metab*. 2017;37(7):2433-2440. doi:10.1177/0271678X16668536

26. Heijtel DFR, Mutsaerts HJMM, Bakker E, et al. Accuracy and precision of pseudo-continuous arterial spin labeling perfusion during baseline and hypercapnia: a head-to-head comparison with ^{15}O H_2O positron emission tomography. *Neuroimage*. 2014;92:182-192. doi:10.1016/j.neuroimage.2014.02.011

27. Puig O, Vestergaard MB, Lindberg U, et al. Phase contrast mapping MRI measurements of global cerebral blood flow across different perfusion states - A direct comparison with 15O-H2O positron emission tomography using a hybrid PET/MR system. *J Cereb Blood Flow Metab*. 2019;39(12):2368-2378. doi:10.1177/0271678X18798762

28. van Golen LW, Kuijer JPA, Huisman MC, et al. Quantification of cerebral blood flow in healthy volunteers and type 1 diabetic patients: comparison of MRI arterial spin labeling and [(15)O]H2O positron emission tomography (PET). *J Magn Reson Imaging*. 2014;40(6):1300-1309. doi:10.1002/jmri.24484

29. Lautt WW. Regulatory processes interacting to maintain hepatic blood flow constancy: Vascular compliance, hepatic arterial buffer response, hepatorenal reflex, liver regeneration, escape from vasoconstriction. *Hepatol Res*. 2007;37(11):891-903. doi:10.1111/j.1872-034X.2007.00148.x

30. Mathie RT. Hepatic blood flow measurement with inert gas clearance. *J Surg Res*. 1986;41(1):92-110. doi:10.1016/0022-4804(86)90014-4

31. Middlekauff HR, Nitzsche EU, Nguyen AH, Hoh CK, Gibbs GG. Modulation of Renal Cortical Blood Flow During Static Exercise in Humans. *Circulation Research*. 1997;80(1):62-68. doi:10.1161/01.RES.80.1.62

32. Nuutila P, Raitakari M, Laine H, et al. Role of blood flow in regulating insulin-stimulated glucose uptake in humans. Studies using bradykinin, [15O]water, and [18F]fluoro-deoxy-glucose and positron emission tomography. *J Clin Invest*. 1996;97(7):1741-1747. doi:10.1172/JCI118601

33. Malminiemi K, Laine H, Knuuti MJ, et al. Acute effects of celiprolol on muscle blood flow and insulin sensitivity: studies using [15O]-water, [18F]-fluorodeoxyglucose and positron emission tomography. *Eur J Clin Pharmacol*. 1997;52(1):19-26. doi:10.1007/s002280050243

34. Heinonen I, Kemppainen J, Kaskinoro K, et al. Effects of adenosine, exercise, and moderate acute hypoxia on energy substrate utilization of human skeletal muscle. *Am J Physiol Regul Integr Comp Physiol*. 2012;302(3):R385-390. doi:10.1152/ajpregu.00245.2011

35. Heinonen I, Kemppainen J, Kaskinoro K, et al. Comparison of exogenous adenosine and voluntary exercise on human skeletal muscle perfusion and perfusion heterogeneity. *J Appl Physiol (1985)*. 2010;108(2):378-386. doi:10.1152/japplphysiol.00745.2009

36. Heinonen I, Boushel R, Hellsten Y, Kalliokoski K. Regulation of bone blood flow in humans: The role of nitric oxide, prostaglandins, and adenosine. *Scand J Med Sci Sports*. 2018;28(5):1552-1558. doi:10.1111/sms.13064

37. Garbarino S, Caviglia G, Sambuceti G, Benvenuto F, Piana M. A novel description of FDG excretion in the renal system: application to metformin-treated models. *Phys Med Biol*. 2014;59(10):2469-2484. doi:10.1088/0031-9155/59/10/2469

38. Hato T, Friedman AN, Mang H, et al. Novel application of complementary imaging techniques to examine in vivo glucose metabolism in the kidney. *American Journal of Physiology-Renal Physiology*. 2016;310(8):F717-F725. doi:10.1152/ajprenal.00535.2015

Tables

TABLE 1 Baseline characteristics of patients (n = 91)

	Variable	Mean (SD)/Median [IQR]/Frequency (Percent)
Demographic factors		
	Age (years)	64.0 [58.5–69.0]
	Male sex	26 (28.6)
	Weight (kg)	83.9 (16.5)
	Height (cm)	168.8 (8.5)
	Body mass index (kg/m^2)	29.4 (4.9)
Cardiovascular risk factors		
	Diabetes mellitus	16 (17.6)
	Current smokers	6 (6.6)
	Previous smokers	37 (40.7)
	Dyslipidaemia	68 (74.7)
	Hypertension	56 (61.5)
	Family history of CAD	40 (44.0)
Medications		
	Anticoagulant	11 (12.1)
	Antiplatelet therapy	28 (30.8)
	Antiarrythmics	2 (2.2)
	Beta-blocker	32 (35.2)
	Calcium channel blocker	28 (30.8)
	Angiotensin-converting enzyme inhibitor	9 (9.9)
	Angiotensin receptor blocker	30 (33.0)
	Diuretic	19 (20.9)
	Long-acting nitrate	8 (8.8)
	Lipid lowering therapy	52 (57.1)

	Anti-diabetic medication	12 (13.2)
	Insulin	5 (5.5)
Coronary artery calcium score (n = 78)		
	Median	69.5 [1.0–206.8]
	0	19 (24.4)
	1-100	28 (35.9)
	100-400	18 (23.1)
	>400	13 (16.7)
Cardiovascular disease history		
	Previous CABG	0 (0)
	Previous PCI	7 (7.7)
	Atrial fibrillation/flutter	11 (12.1)
	Dialysis	0 (0)
	Pacemaker	4 (4.4)
Blood pressure and heart rate (n = 88)		
	Systolic blood pressure at rest	136.0 (21.4)
	Diastolic blood pressure at rest	71.1 (12.5)
	Heart rate at rest	66.5 (11.6)
	Systolic blood pressure at 3 min stress	133.4 (23.1)
	Diastolic blood pressure at 3 min stress	66.1 (13.5)
	Heart rate at 3 min stress	87.4 (14.4)

CABG = coronary artery bypass graft, PCI = percutaneous coronary intervention

TABLE 2 Myocardial blood flow (MBF) in the left ventricular myocardium globally and in each main coronary artery territory

	Rest MBF, mL/min/g	Stress MBF, mL/min/g	Stress/Rest ratio (reserve)	p-value (rest vs. stress)

Global	1.01 [0.90–1.22]	3.47 [3.06–3.95]	3.28 [2.91–3.67]	<0.0001
LAD	1.07 [0.90–1.28]	3.58 [3.01–3.88]	3.08 [2.77–3.59]	<0.0001
LCX	1.01 [0.91–1.20]	3.61 [3.18–4.11]	3.46 [2.99–3.82]	<0.0001
RCA	0.90 [0.79–1.09]	3.34 [2.77–3.76]	3.35 [2.91–4.00]	<0.0001

LAD = left anterior descending artery, LCX = left circumflex artery, RCA = right coronary artery

Values are median (IQR). P-value is for paired comparison between rest and stress.

TABLE 3 Perfusion at rest and during stress in different organs

Organ	**Rest flow, mL/min/mL**	**Stress flow, mL/min/mL**	**Stress/Rest ratio (reserve)**	**Stress-rest difference (delta), mL/min/mL**	**p-value**
Whole brain	0.43 [0.38–0.48]	0.32 [0.28–0.35]	0.74 [0.68–0.81]	-0.11 [-0.14 – -0.08]	<0.0001
White matter	0.29 [0.26–0.33]	0.25 [0.21–0.27]	0.83 [0.77–0.89]	-0.05 [-0.07– -0.03]	<0.0001
Brain cortical grey matter	0.44 [0.39–0.49]	0.33 [0.29–0.35]	0.73 [0.69–0.79]	-0.11 [-0.14 – -0.09]	<0.0001
Spleen	1.11 [0.97–1.30]	0.31 [0.23–0.40]	0.29 [0.20–0.38]	-0.80 [-0.92 – -0.64]	<0.0001
Kidney	0.87 [0.75–1.00]	0.65 [0.49–0.76]	0.77 [0.61–0.91]	-0.19 [-0.35– -0.07]	<0.0001
Liver	1.10 [0.83–1.82]	3.32 [1.79–5.41]	2.49 [1.31–4.47]	1.83 [0.35–4.04]	<0.0001

Pancreas	0.87 [0.72–1.05]	0.87 [0.73–1.11]	1.04 [0.89–1.22]	0.04 [-0.10–0.19]	0.14
Colon	0.09 [0.08–0.12]	0.13 [0.10–0.17]	1.37 [1.03–1.74]	0.04 [0.01–0.07]	<0.0001
Duodenum	0.37 [0.27–0.48]	0.53 [0.42–0.65]	1.37 [1.18–1.72]	0.15 [0.06–0.23]	<0.0001
Skeletal muscle	0.07 [0.05–0.09]	0.04 [0.03–0.06]	0.59 [0.46–0.88]	-0.03 [-0.04–0.00]	<0.0001
Bone	0.03 [0.03–0.05]	0.03 [0.02–0.03]	0.69 [0.57–0.95]	-0.01 [-0.02–0.00]	<0.0001

Values are median (IQR). P-value is for paired comparison between rest and stress.

Figures

Figure 1.

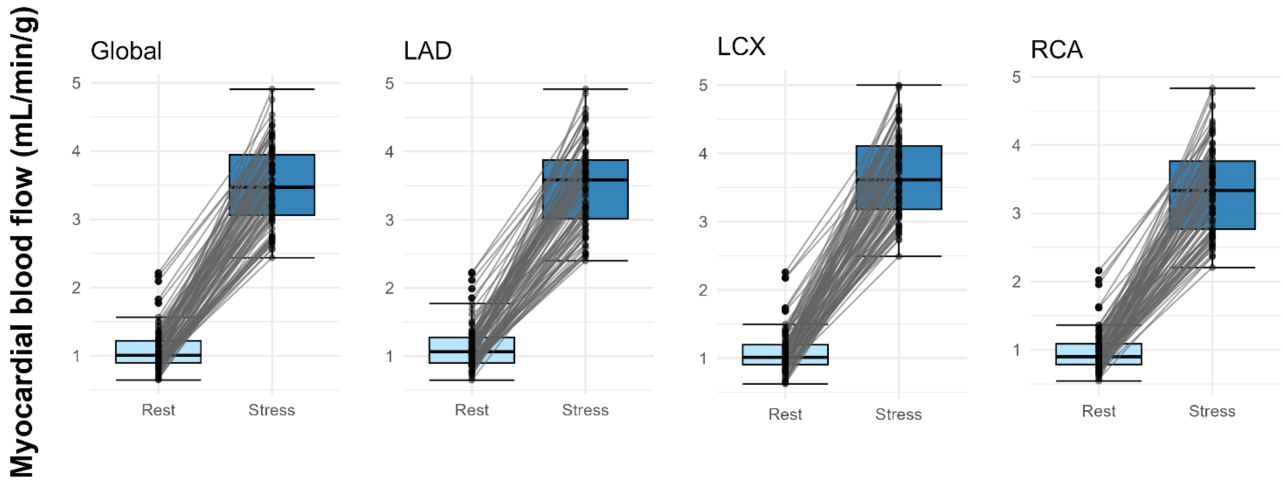

Myocardial blood flow (mL/min/g)
Global
LAD
LCX
RCA
5
4
3
2
1
Rest
Stress

Figure 2.

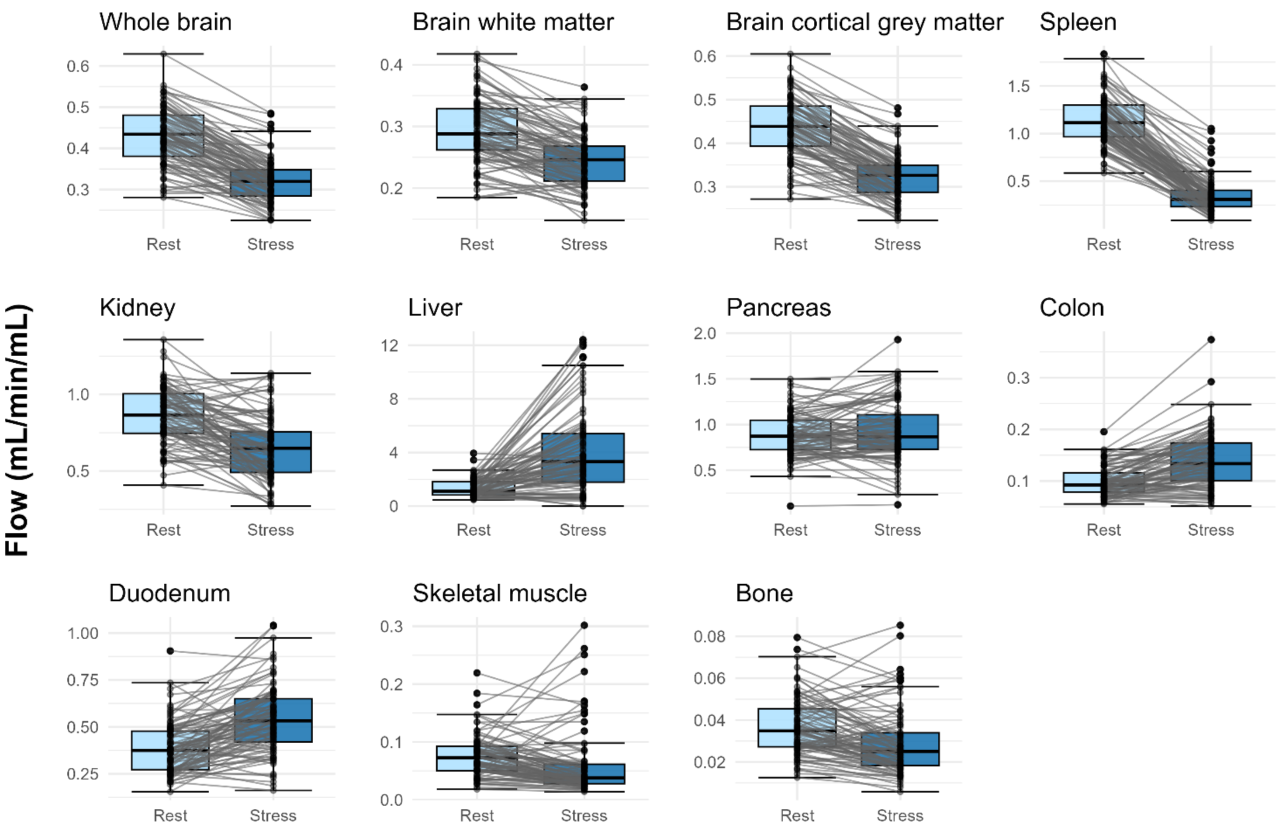

Figure legends

Figure 1. Myocardial blood flow (MBF) at rest and during adenosine stress in the whole left ventricular myocardium and in each main coronary artery territory

Figure 2. Perfusion (flow) values in different organs at rest and during adenosine stress